Arch. Metall. Mater. **70** (2025), 4, 1753-1758

DOI: https://doi.org/10.24425/amm.2025.156258

N.S.M. ZAIMI[1], M.A.A.M. SALLEH[2*], M.F.H. BASER[2], N.A.I. BAHARIN[2],
M.S.A. AZIZ[1], M.M. AL B. ABDULLAH[2], M. NABIAŁEK[3]

IMPACT OF BISMUTH AS MICROALLOYING ELEMENT IN Sn-0.7Cu LEAD-FREE SOLDER ALLOYS

This study investigated the impact of different amounts of bismuth (Bi) (0 wt.%, 0.5 wt.%, 1.0 wt.%, 1.5 wt.%, and 2.0 wt.%) on the microstructure and mechanical properties of Sn-0.7Cu solder, which is known for its high strength. The microstructure analysis was carried out using an optical microscope (OM). A single lap shear test was carried out to evaluate the shear strength of the solder alloys. The results demonstrated that the addition of 1.5 wt.% Bi effectively refined the formation of Cu_6Sn_5 intermetallic in the solder joint compared to Sn-0.7Cu/Cu joints. Additionally, the incorporation of 1.5 wt.% Bi led to a substantial increase in shear strength compared to pure Sn-0.7Cu. These findings validate the potential application of the developed material as a high-strength solder for advanced interconnecting purposes.

Keywords: Lead-free solder; Bismuth; Intermetallic; Microstructure; Shear

1. Introduction

Solder alloys are critical in ensuring the reliability, functionality, and structural integrity of electronic packages. Traditionally, tin-lead (Sn-Pb) solder alloys were widely utilized in electronics for joining components to substrates, owing to their exceptional properties [1,2]. These alloys offer a low melting point of 183°C, excellent wettability, robust mechanical strength, and affordability, making them highly effective for electronic applications [3-5]. The inclusion of Pb in solder alloys presents serious health and environmental challenges due to its high toxicity. In response, many countries have implemented stringent regulations to restrict or ban lead in solder materials. This has driven a global shift toward the development of lead-free alternatives as safer and more sustainable solutions.

Among those lead-free alternatives, Sn-0.7Cu solder alloys have gained more attention due to the cost effectiveness, safer and more sustainable solutions [6,7]. However, several challenges arise related to Sn-0.7Cu solder alloys. One of the major challenges associated with these alloys is the formation of a coarse microstructure in the bulk solder alloy and at the interface [8,9]. To address these challenges, microalloying with metal elements has been explored. Shelaby et al. [10], incorporated several alloying elements, such as In and Cr, into Sn-0.7Cu solder alloys. It was reported that the addition of In and Cr suppressed the formation of eutectic Sn-Cu phases [10]. Then, P. Yi et al. [11] has successfully explored the effect of Nd alloying element in Sn-Ag-Cu solder alloys. It was found that, the size of b-Sn was reduced with addition of Nd as compared to pure Sn-Ag-Cu solder alloys. Along with that, the eutectic phases increased with increasing amount of Nd content, resulting from reduction in the size of IMCs. Additionally, Ragab et al. [12] attempted to incorporate antimony (Sb) into Sn-6.5Zn-0.3Cu solder alloys. Their findings indicated that the addition of Sb successfully resulted in a uniform dispersion of intermetallic compounds (IMCs) such as γ-Cu_5Zn_8 and Sb_2SnZn, alongside ethe α-Zn and β-Sn matrix. This led to a refinement of the microstructure and also increased the creep resistance of the solder alloys.

In this study, we aimed to investigate the effects of bismuth (Bi) addition on the intermetallic layer and mechanical properties of Sn-0.7Cu solder alloys. Five different solder alloys were prepared with varying amounts of Bi: Sn-0.7Cu (SC), Sn-0.7Cu-0.5Bi (SC-0.5Bi), Sn-0.7Cu-1.0Bi (SC-1.0Bi), Sn-0.7Cu-1.5Bi (SC-1.5Bi), and Sn-0.7Cu-2.0Bi (SC-2.0Bi). The microstructure formation and shear strength properties of these alloys were then systematically evaluated.

[1] UNIVERSITI SAINS MALAYSIA, SCHOOL OF MECHANICAL ENGINEERING, ENGINEERING CAMPUS, 14300 NIBONG TEBAL, PENANG, MALAYSIA
[2] UNIVERSITI MALAYSIA PERLIS (UNIMAP), FACULTY OF CHEMICAL ENGINEERING AND TECHNOLOGY, CENTER OF EXCELLENCE GEOPOLYMER & GREEN TECHNOLOGY (CEGEOGTECH), TAMAN MUHIBBAH, 02600 JEJAWI, ARAU, PERLIS, MALAYSIA
[3] CZESTOCHOWA UNIVERSITY OF TECHNOLOGY, FACULTY OF PRODUCTION ENGINEERING AND MATERIALS TECHNOLOGY, DEPARTMENT OF PHYSICS, 19 ARMII KRAJOWEJ AV., 42-200 CZĘSTOCHOWA, POLAND

* Corresponding author: arifanuar@unimap.edu.my

© 2025. The Author(s). This is an open-access article distributed under the terms of the Creative Commons Attribution License (CC-BY 4.0). The Journal license is: https://creativecommons.org/licenses/by/4.0/deed.en. This license allows others to distribute, remix, modify, and build upon the author's work, even commercially, as long as the original work is attributed to the author.

2. Experimental procedure

2.1. Sample preparation

In this study, Sn-0.7Cu (SC) solder alloys were purchased from Nihon Superior, Osaka, Japan, while bismuth (Bi) was obtained from Sigma Aldrich (M) Sdn. Bhd., Selangor, Malaysia. Sn-0.7Cu–xBi (SC–xBi) solder alloys were prepared through the casting process. The SC solder alloys, with varying weight percentages (wt.%) of Bi (ranging from 0 to 2.0 wt.%), were melted in an electric-resistance furnace at a temperature of 350°C for one hour. The mixture was then stirred to ensure homogeneity before being poured into a pre-heated stainless-steel mold and allowed it to cool and solidify at room temperature. To prepare a ~900 µm solder ball, the cast solder alloys were cold rolled into a thin sheet and then punched into disc shapes. These disc shapes were subsequently dipped in a rosin mildly activated (RMA) flux and melted in a reflow oven at a temperature of 250°C. The resulting solder balls were then subjected to a series of sieves to achieve a uniform size of solder ball.

2.2. Microstructure analysis

Solder ball joints were prepared by placing a ~900 µm solder ball on a Cu substrate, followed by the application of rosin mildly activated (RMA) flux prior to the reflow soldering process in a reflow oven. Afterward, the solder joints were cold-mounted using epoxy resin and ground with a series of SiC papers. This was followed by mechanical polishing using alumina solutions of 1.0 and 0.3 µm. Finally, an OPS solution was used for further polishing to achieve even clearer observations of the microstructure. The microstructure of SC-xBi solder joints were then observed using an optical microscope. Then, the thickness of intermetallic compound (IMC) layer was measured by dividing the area (A) of IMC layer by its length (L). For each composition of the SC-xBi solder joints, the average value from five samples was reported.

2.3. Lap-shear testing

To evaluate the shear strength of SC-xBi solder joints, a single lap shear test was performed using a Universal Testing Machine (UTM) from Instron at room temperature, with a crosshead speed of 5 mm/min. For each composition of the SC-xBi solder joints, the average value from five samples was reported. The specifications for the Cu substrate adhered to the ASTM D1002 standard as indicates in Fig. 1.

3. Results and discussions

3.1. Phase diagram of Sn-0.7Cu-xBi alloy and solidification path

The SC-xBi system phase diagram was generated using Thermo-Calc 2022a and the TCSLD 3.3 database, as depicted in Fig. 2. The diagram indicates a gradual decrease in the liquidus temperature with increasing Bi content. For low Bi concentrations (0.5-1.0 wt.%), the liquid phase coexists with the βSn phase over a broad temperature range. The eutectic reaction, involving the liquid phase transitioning into β-Sn and ηCu_6Sn_5, occurs at a slightly reduced temperature with increasing Bi content. This depression of the liquidus line is attributed to the dissolution of Bi into the Sn-rich phase, which alters the thermodynamic equilibrium of the system.

Fig. 3 illustrates the simulated solidification sequence under Scheil conditions for the SC-xBi system and the phase sequences were summarized in TABLE 1. The solidification path phase sequences vary with the addition of Bi in the SC solder alloy. For the base SC alloy, the solidification begins with the formation of βSn at 228°C, followed by the formation of ηCu_6Sn_5 as a secondary phase, with solidification complete at 226.9°C. The narrow temperature range for SC base alloy highlights a relatively straightforward with limited phase transitions due to eutectic solidification. When Bi is introduced at 0.5 wt.%, the onset temperature decreases slightly to 227°C, and

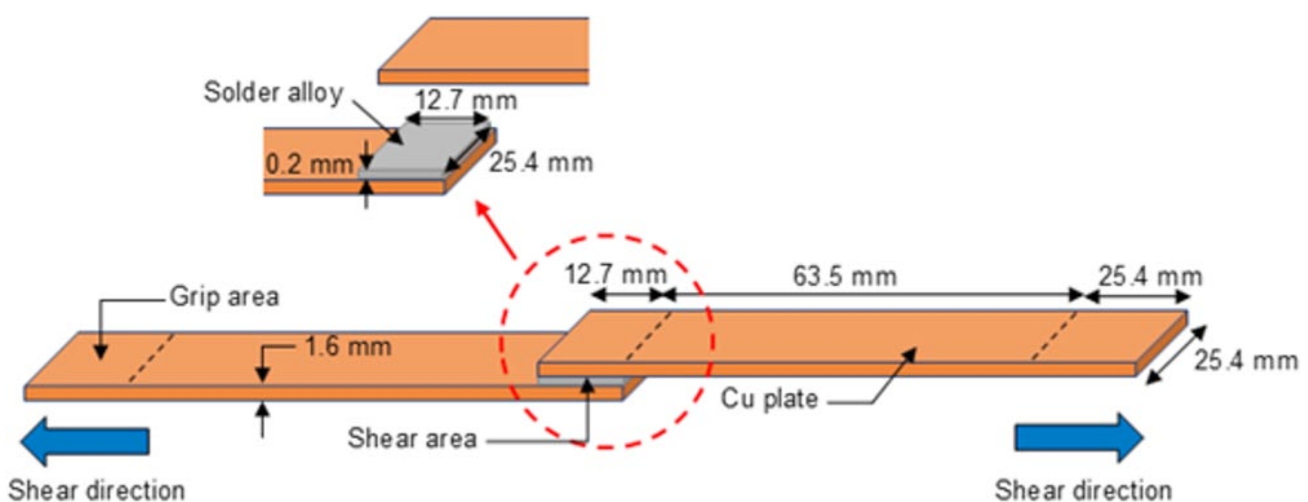

Fig. 1. Dimensions of the single lap shear test specimen are specified in accordance with the ASTM D1002 standard

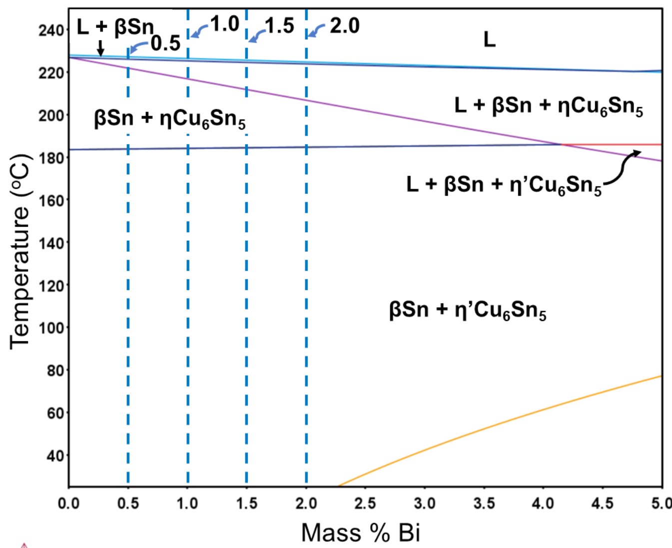

Fig. 2. Phase diagram of the SC-xBi solder alloy

the final solidification temperature drops significantly to 195°C, indicating an extended solidification range. The solidification sequence remains dominated by βSn formation, followed by the coexistence of βSn and ηCu_6Sn_5. This suggests that the introduction of Bi alters the thermal equilibrium, likely by modifying the solubility of Cu and Sn, which extends the solidification process.

A similar effect on solidification was reported by Ali et al. [13] following the addition of Bi into SAC alloys. Notably, a new phase, $\eta' Cu_6Sn_5$, begins to form at lower temperatures, as illustrated in Fig. 3(c-e), highlighting the increasing influence of Bi on the stabilization and transformation of intermetallic compounds (IMCs). The solidification pathway becomes more complex, involving the coexistence of βSn, $\eta' Cu_6Sn_5$, and Bi phases after addition of 1.5 wt.% and 2.0 wt.% of Bi as shown in Fig. 3(d-e). This extended temperature range indicates that Bi significantly affects the solidification dynamics by delaying the completion of solidification.

Fig. 3. Scheil solidification sequences in SC-xBi; (a) SC, (b) SC-0.5Bi, (c) SC-1.0Bi, (d) SC-1.5Bi and (e) SC-2.0Bi

TABLE 1

The temperature solidification sequence of the SC and SC-xBi solder alloys

Composition	Liquid + βSn (°C)	ηCu_6Sn_5 (°C)	η'Cu_6Sn_5 (°C)	η'Cu_6Sn_5 + Bi (°C)
Sn-0.7Cu	228	226.9	—	—
Sn-0.7Cu-0.5Bi	227	226	—	—
Sn-0.7Cu-1.0Bi	226.5	225.4	185.7	—
Sn-0.7Cu-1.5Bi	225.7	224.7	186	138.4
Sn-0.7Cu-2.0Bi	224.9	224.7	186	138.4

3.2. Microstructural analysis

During the solidification process, an intermetallic compound (IMC) was formed at the interface between the solder and the Cu substrates. Fig. 4(a-e) depicts the cross-sectional image of IMC layer that are formed at the interface between solder materials and Cu substrate varying with different weight percentage (wt.%) of Bi. The interfacial reaction between SC-xBi solder alloys and Cu substrate, lead to the formation of Cu_6Sn_5 IMC. In this research, no formation of Cu_3Sn can be observed.

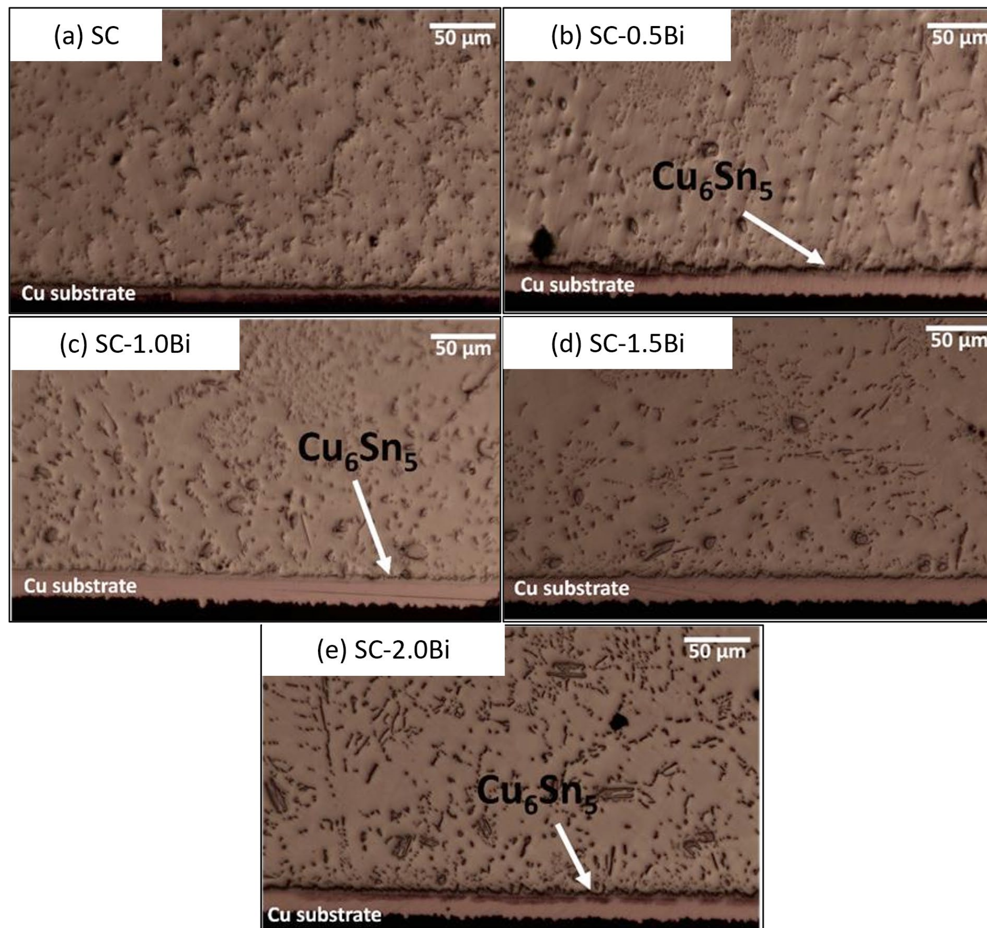

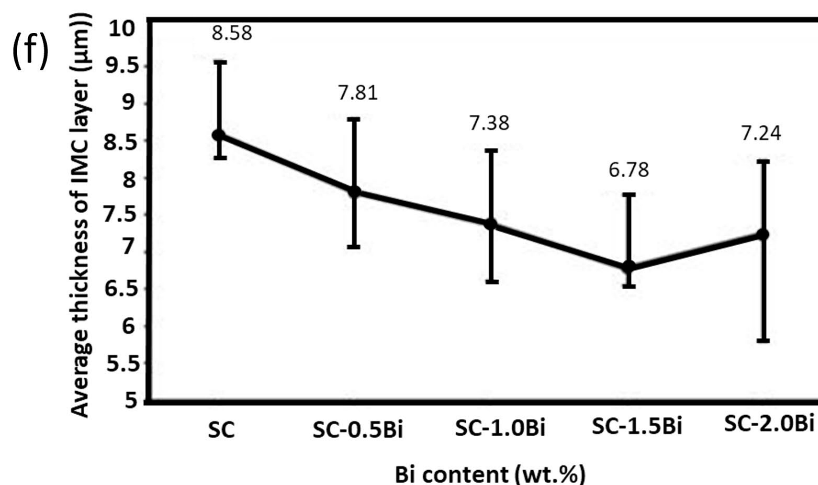

Fig. 4. The cross-sectioned image of SC-xBi at the interfacial IMC for (a) SC, (b) SC-0.5Bi, (c) SC-1.0Bi, (d) SC-1.5Bi, (e) SC-2.0Bi and (f) Average thickness of IMC layer

Cu_3Sn commonly forms in Sn-Cu solder joint during subsequent ageing process. During the soldering and solidification process of Sn-Cu solder joints, Cu_6Sn_5 IMCs will be formed results from the dissolution of Cu from the Cu substrates. According to the phase diagram in Fig. 2, Cu_6Sn_5 forms as a direct reaction product between Cu and liquid Sn at 226.9°C. Meanwhile, for interfacial IMC of Cu_3Sn, it can only be produced through a solid-state reaction between Cu and Cu_6Sn_5 [14].

Fig. 4(f) shows a bar graph depicting the average thickness of IMC layer that was measured using Image-J software. Based on Fig. 4(f) it was observed that; the average thickness of IMC layer was increased with increasing amount of Bi. Specifically, the addition of 1.5 wt.% of Bi to SC solder alloys resulted in the thinnest IMC layer, exhibiting a reduction of approximately 21% compared to pure SC solder alloys. However, the addition of 2.0 wt.% Bi resulted in a slight increase in the thickness of the IMC layer although it still remained thinner than that of pure SC solder alloys. The improvement in the average thickness of IMC layer may due to the effect of Bi addition in SC solder alloys. As reported by Y. Chen et.al [15], the dissolved Bi in the Sn matrix may increase the atomic diffusion barrier and reduce the interdiffusion rate of Cu and Sn atoms, hence resulted in the thinner IMC layer of SC-xBi solder alloys. Therefore, the proportion of Bi added should be controlled within an appropriate range to ensure optimal performance of SC solder alloys.

3.3. Shear strength analysis

Solder joints are frequently exposed to mechanical stress in actual operating conditions. To investigate the impact of various weight percentage (wt.%) of Bi to the reliability of SC solder alloys, a single lap-shear test was conducted. Fig. 5 depicts the bar graph that represents the average shear strength with respect to different wt.% of Bi content. From the bar graph Fig. 5, it can be observed that, the average shear strength increased with increasing amount of Bi. The maximum average shear strength was obtained with 1.5 wt.% Bi, reaching 8.48 MPa. This represents a 51% improvement over pure Sn-0.7Cu solder joints. However, addition of Bi beyond 2.0 wt.% could reduce the shear strength of SC solder alloys. Nonetheless, the average shear strength with 2.0 wt.% Bi remains higher than pure SC solder alloys.

The improvement in the average shear strength of SC solder alloys with the addition of Bi up to 1.5 wt.% can be attributed to the solid solution strengthening effect. The presence of Bi atoms into the Sn matrix promotes solid solution strengthening by dissolving within the Sn structure. This dissolution increases the alloy's resistance to dislocation movement, thereby improving the overall strength and mechanical properties of the solder joint. Furthermore, this dissolution also may lead to increase in the lattice parameter "a" and "c" which could enhance the anisotropy of Sn crystal structure, as reported by Nogita et al. [16]. The resulting local nonuniformity in the lattice due to the alloying elements make plastic deformation more challenging by restricting the dislocation motion in the SC solder alloys [16]. Therefore, the complex relationship between incorporation of Bi and lattice structure contributes to the improvement in the shear strength of SC solder alloys. However, excess Bi addition beyond 2.0 wt.% has been observed to reduce the shear strength of SC alloys. This phenomenon occur may due to the excess Bi atoms have been forced out of solution during cooling, leading to the formation of a second phase of Bi precipitates. Consequently, it can be inferred that from this study incorporating more than 2.0 wt.% Bi does not provide any additional strengthening effect to the SC solder alloys. In contrast, Liu et al. [17] reported that, incorporation of Bi beyond 4 wt.% to Sn-3Ag-Cu could compromised the shear strength of the solder alloys due to the brittleness of Bi precipitates, ultimately leading to brittle failure.

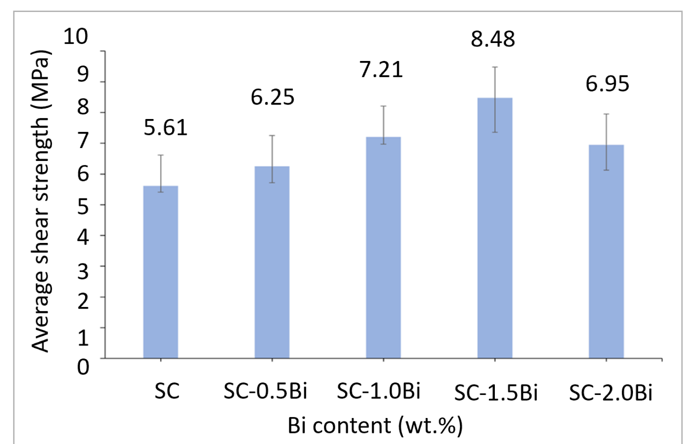

Fig. 5. Bar graph illustrates the average shear strength of SC-xBi solder alloys

4. Conclusions

The study presents a detailed analysis of microstructural modifications, phase formations, mechanical behavior, and thermal properties induced by bismuth addition in the range of 0 to 2.0 wt.% Bi, highlighting its potential to enhance solder performance. Several conclusions can be drawn from this study:

i. As according to the phase diagram and the simulated solidification sequence under Scheil conditions generated from Thermo-Calc software, the solidification path phase sequences vary with the addition of Bi in the SC solder alloy.
ii. In the SC-xBi solder joint, the additions of 1.5 wt.% of Bi showing the lowest thickness of interfacial IMC with 21% reduction as compared to the SC solder alloys. The reduction in the thickness of IMC layer in SC-1.5 Bi was due to the effect of Bi that may reduce the interdiffusion rate of Cu and Sn atoms.
iii. Additions of different wt.% of Bi increased the average shear strength of SC solder alloys. The results proved that the additions of 1.5 wt.% Bi exhibited highest average shear strength due to the solid solution strengthening mechanism.

In the future, investigations into the microstructural evolution during extended thermal cycling can provide deeper insights into phase stability and mechanical performance, as well as predict the impact of Bi microalloying on solder performance.

REFERENCES

[1] N.S. Mohamad Zaimi et al., Effect of kaolin geopolymer ceramic addition on the properties of Sn-3.0Ag-0.5Cu solder joint. Mater. Today Commun. **25**, 101469 (2020). DOI: https://doi.org/10.1016/j.mtcomm.2020.101469

[2] Y. Wen et al., Reliability enhancement of Sn-1.0Ag-0.5Cu nano-composite solders by adding multiple sizes of TiO2nanoparticles. J. Alloys Compd. **696**, 799-807 (2017). DOI: https://doi.org/10.1016/j.jallcom.2016.12.037

[3] M.N. Zulkifli, I. Abdullah, N.H. Azhan, A. Jalar, Micromechanical and microstructure evolution of leaded (SnPb) and lead-free (SAC305 and SnCu) mixed solder joints during isothermal aging. J. Adhes. Sci. Technol. **38**, 20, 3842-3859 (2024). DOI: https://doi.org/10.1080/01694243.2024.2356962

[4] N.S.M. Zaimi et al., Performance of Sn-3.0Ag-0.5Cu Composite Solder with Kaolin Geopolymer Ceramic Reinforcement on Microstructure and Mechanical Properties under Isothermal Ageing. Materials (Basel) **14**, 4, 776 (2021). [Online]. Available: https://www.mdpi.com/1996-1944/14/4/776

[5] N.S.M. Zaimi et al., Effect of Kaolin Geopolymer Ceramics Addition on the Microstructure and Shear Strength of Sn-3.0Ag-0.5Cu Solder Joints during Multiple Reflow. Materials (Basel) **15**, 8 (2021). DOI: https://doi.org/10.3390/MA15082758

[6] P.D. Sonawane, V.K. Bupesh Raja, M. Gupta, Mechanical properties and corrosion analysis of lead-free Sn-0.7Cu solder CSI joints on Cu substrate. Mater. Today Proc. **46**, 1101-1105 (2021). DOI: https://doi.org/10.1016/j.matpr.2021.01.521

[7] G.A. Lee, A. Sharma, J.P. Jung, Electrochemical deposition of Sn-0.7Cu alloy modified with nano-WO3 for high-density mini-LED packaging. J. Mater. Sci. Mater. Electron. **35**, 14, 953 (2024). DOI: https://doi.org/10.1007/s10854-024-12606-4

[8] X. Hu, Y. Lai, X. Jiang, Y. Li, Effects of In addition on the wettability, interfacial characterization and properties of ternary Sn–Cu–Ni solders. J. Mater. Sci. Mater. Electron. **29**, (2018). DOI: https://doi.org/10.1007/s10854-018-0009-x

[9] S.M. Abdelaziz, H.Y. Zahran, A.F. Abd El-Rehim, M. Abd El-Hafez, Effects of trace addition of Fe on the thermal, microstructure, and tensile creep properties of Sn-0.7Cu eutectic alloy. J. Mater. Sci. Mater. Electron. **35**, 12, 837 (2024). DOI: https://doi.org/10.1007/s10854-024-12478-8

[10] R. M. Shalaby, Indium, chromium and nickel-modified eutectic Sn–0.7 wt% Cu lead-free solder rapidly solidified from molten state. J. Mater. Sci. Mater. Electron. **26**, 9, 6625-6632 (2015). DOI: https://doi.org/10.1007/s10854-015-3261-3

[11] P. Yi et al., Effect of Nd addition on the corrosion behavior of SAC305 solder alloy. Corros. Sci. **220**, 111264 (2022). DOI: https://doi.org/10.1016/j.corsci.2023.111264

[12] M. Ragab, H. Alsnani, A.E. Hammad, A.S. Abd-Elrahman, The role of Sb on the microstructure and creep behaviors of Sn–6.5Zn–0.3Cu Pb-free solder alloy. J. Mater. Sci. Mater. Electron. **35**, 26, 1-11, (2024). DOI: https://doi.org/10.1007/s10854-024-13421-7

[13] H.E. Ali, A.M. El-Taher, H. Algarni, Influence of bismuth addition on the physical and mechanical properties of low silver/lead-free Sn-Ag-Cu solder. Mater. Today Commun. **39**, 109113 (2024). DOI: https://doi.org/10.1016/j.mtcomm.2024.109113

[14] M.I.I. Ramli et al., Influence of 1.5 wt.% bi on the microstructure, hardness, and shear strength of sn-0.7cu solder joints after isothermal annealing. Materials (Basel) **14**, 18 (2021). DOI: https://doi.org/10.3390/ma14185134

[15] Y. Chen, Z.C. Meng, L.Y. Gao, Z.Q. Liu, Effect of Bi addition on the shear strength and failure mechanism of low-Ag lead-free solder joints. J. Mater. Sci. Mater. Electron. **32**, 2, 2172-2186 (2021). DOI: https://doi.org/10.1007/s10854-020-04982-4

[16] K. Nogita et al., Effects of Bismuth in Sn-Cu Based Solder Alloys and Interconnects. pp. 1-7 (2017).

[17] Y. Liu, F. Sun, X. Li, Effect of Ni, Bi concentration on the microstructure and shear behavior of low-Ag SAC-Bi-Ni/Cu solder joints. J. Mater. Sci. Mater. Electron. **25**, 6, 2627-2633 (2014). DOI: https://doi.org/10.1007/s10854-014-1921-3